

Urban Spatiotemporal Data Synthesis via Neural Disaggregation

Bin Han
bh193@uw.edu
University of Washington
Seattle, USA

Bill Howe
billhowe@uw.edu
University of Washington
Seattle, USA

ABSTRACT

The level of granularity of open data often conflicts the benefits it can provide. Less granular data can protect individual privacy, but to certain degrees, sabotage the promise of open data to promote transparency and assist research. Similar in the urban setting, aggregated urban data at high-level geographic units can mask out the underline particularities of city dynamics that may vary at lower areal levels. In this work, we aim to synthesize fine-grained, high resolution urban data, by breaking down aggregated urban data at coarse, low resolution geographic units. The goal is to increase the usability and realize the values as much as possible of highly aggregated urban data. To address the issue of simplicity of some traditional disaggregation methods – 1) we experimented with numerous neural-based models that are capable of modeling intricate non-linear relationships among features. Neural methods can also leverage both spatial and temporal information concurrently. We showed that all neural methods perform better than traditional disaggregation methods. Incorporating the temporal information further enhances the results. 2) We proposed a training approach for disaggregation task, Chain-of-Training (COT), that can be incorporated into any of the training-based models. COT adds transitional disaggregation steps by incorporating intermediate geographic dimensions, which enhances the predictions at low geographic level and boosts the results at higher levels. 3) We adapted the idea of reconstruction (REC) from super-resolution domain in our disaggregation case – after disaggregating from low to high geographic level, we then re-aggregate back to the low level from our generated high level values. Both strategies improved disaggregation results on three datasets and two cities we tested on.

CCS CONCEPTS

• **General and reference** → **Empirical studies**; • **Computing methodologies** → **Computer vision**; • **Applied computing**;

KEYWORDS

urban computing, spatial disaggregation

ACM Reference Format:

Bin Han and Bill Howe. 2023. Urban Spatiotemporal Data Synthesis via Neural Disaggregation. In *Proceedings of ACM Conference (Conference'17)*. ACM, New York, NY, USA, 7 pages. <https://doi.org/10.1145/nnnnnnn.nnnnnnn>

1 INTRODUCTION

High-quality, longitudinal, and freely available urban data, coupled with advances in machine learning, improve our understanding and management of urban environments [6]. Over the last two decades, cities have increasingly released datasets publicly on the web, proactively, in response to transparency regulation. For example, in the US, all 50 states and the District of Columbia have passed some version of the federal Freedom of Information (FOI) Act. While this first wave of open data was driven by FOI laws and made national government data available primarily to journalists, lawyers, and activists, a second wave of open data, enabled by the advent of open source and web 2.0 technologies, was characterized by an attempt to make data “open by default” to civic technologists, government agencies, and corporations [13].

While making data publicly available possesses numerous benefits, such as enabling extensive analyses of urban dynamics or assisting policymakers in making urban development decisions [14, 16], however, the open data might contain sensitive information about individuals. Consequently, sharing such data at the individual level imposes potential risks to individual privacy. For example, starting in 2017, NYC open data portal no longer released longitudes and latitudes of taxi trips. Instead, they released the central point of the geographic regions where the taxi trips started and ended.

The level of granularity of open data often conflicts the benefits it can provide. As stated in [5], less granular data can protect individual privacy, but to certain degrees, sabotage the promise of open data to promote transparency and assist research. For instance, in population disaggregation studies, highly aggregated population counts at large, coarse areal units can hide critical local hotspots and trends, by smoothing out the spatial variations [7]. Similar in the urban setting, aggregated urban data at high-level geographic units can mask out the underline particularities of city dynamics that may vary at lower areal levels. Additionally, the predefined geographic units could often mismatch with the units that users would like to work with for certain type of analyses, not to mention that the boundaries of those pre-defined units could also change overtime.

In this paper, we aim to synthesize fine-grained, high resolution urban data, by breaking down aggregated urban data at coarse, low resolution geographic units. The goal is to increase the usability and realize the values as much as possible of highly aggregated urban data. Traditional spatial disaggregation methods, such as areal weighting and dasymetric mapping, are frequently used in the task.

Permission to make digital or hard copies of all or part of this work for personal or classroom use is granted without fee provided that copies are not made or distributed for profit or commercial advantage and that copies bear this notice and the full citation on the first page. Copyrights for components of this work owned by others than ACM must be honored. Abstracting with credit is permitted. To copy otherwise, or republish, to post on servers or to redistribute to lists, requires prior specific permission and/or a fee. Request permissions from permissions@acm.org.
Conference'17, July 2017, Washington, DC, USA

© 2023 Association for Computing Machinery.
ACM ISBN 978-x-xxxx-xxxx-x/YY/MM... \$15.00
<https://doi.org/10.1145/nnnnnnn.nnnnnnn>

Areal weighting is a simple method that requires no auxiliary information. It is operated under relatively simple assumptions, thus hindering its capacities to achieve great disaggregation performances. Dasymetric mapping methods are popular and leverage auxiliary information to conduct weighted disaggregation. Machine learning and deep learning approaches could be incorporated within to enhance the performances. However, dasymetric mapping methods are highly reliant on auxiliary data, which are often not available in urban setting. The quality of results are also highly dependent on the relevance between auxiliary data and the source data.

To address the issue of simplicity of some traditional disaggregation methods, we experimented with numerous neural-based models that are capable of modeling intricate non-linear relationships among features. Neural methods can also leverage both spatial and temporal information concurrently. We showed that all neural methods perform better than traditional disaggregation methods. To enhance the disaggregation results of neural methods, we proposed a training strategies that can be adopted by any training-based methods – *COT-REC*: chain-of-training with reconstruction. *COT* adds transitional disaggregation steps by incorporating intermediate geographic dimensions, which enhances the predictions at low geographic level and boosts the results at higher levels. We adapted the idea of reconstruction (*REC*) from super-resolution domain in our disaggregation case – after disaggregating from low to high geographic level, we then re-aggregate back to the low level from our generated high level values. Both strategies improved disaggregation results almost all disaggregation tasks we tested.

In summary, we make the following contributions:

- We leveraged neural methods to break down aggregated urban data, which outperformed traditional, simple disaggregation methods that are performed under simple assumptions. We tested neural methods on four different datasets covering different domains and grids.
- We proposed a training strategy – *COT-REC*. *COT-REC* adds transitional steps in disaggregation steps, which enforces better results at lower geographic levels thus enhancing higher level disaggregation results. *COT-REC* provides better results on almost all disaggregation tasks we experimented on.

2 RELATED WORK

Our work is in align with the domain of spatial disaggregation, which is a process to transform values from a spatial scale at low resolution into higher resolution. It is widely used in population studies [10, 15], as well as in other areas, such as disease mapping [1] and vaccination coverage [12].

The most basic approach for spatial disaggregation is areal weighting (*AW*), which breaks down the source value uniformly over the total number of target regions. No auxiliary information is needed for this method, but the assumption of homogeneity is implied – the values are evenly distributed among the target regions [4]. Even though this method is quite simple, in the absence of auxiliary information to help with the disaggregation task, it remains to be a valid and valuable approach. Pycnophylactic interpolation (*PI*), which was first introduced by Tobler in 1979, works similar as areal weighting, but with slight refinement and operates under different assumption. *PI* distributes the values from source regions

onto target regions in an iterative manner, aiming to avoid sharp discontinuity between the target regions while to still preserve the total counts in the source regions. Each iteration will adjust the value for each target zone by considering the weighted average of its nearest neighbors, which ensures the smooth boundaries.

Dasymetric mapping/interpolation/weighting (*DM*) approach is highly popular in the domain of spatial disaggregation. Unlike areal weighting scheme, dasymetric mapping uses auxiliary information to generate a weighted distribution of source values onto the target regions. Recent methods leveraged machine learning approaches to model the relationships between auxiliary data and source values and determine the weights for disaggregation [8–11]. Some previously used auxiliary information include satellite images [11], 3D building information [10], mobile phone usage data [3], terrain elevation and human settlement [8] etc.

Despite the popularity of dasymetric mapping methods in spatial disaggregation, there are several potential limitations of them [2]. They are highly dependent on the availability of auxiliary variables, which are not always available (e.g., remote sensing images or land type data in population disaggregation tasks). Additionally, the quality of the auxiliary information and the relevance between the auxiliary data and source values have great impacts on the disaggregation performances.

3 DATASETS

We worked with four datasets: NYC taxi data, NYC bikeshare data, NYC 911 call data, and Chicago taxi data. Each dataset contains records at the individual level (e.g., individual taxi/bikeshare trip; individual 911-call location). Those four datasets cover various domains and city grids.

- **NYC Taxi Data:** NYC taxi trip data were collected from NYC Open Data portal¹ from 01/01/2016 to 06/30/2016. The raw data are presented in tabular format. Each record summarizes the information for one single taxi trip, which contains the longitude and latitude of the location where the taxi took off.
- **NYC Bikeshare Data:** NYC bikeshare data were collected from NYC DOT² 01/01/2021 to 06/30/2021. Similar to the taxi data, the raw data are presented in tabular format. Each data point summarizes the information for one single bike trip, including the longitude and latitude of the location where the bike was unlocked.
- **NYC 911 Call Data:** NYC 911 call data were collected from NYC Open Data portal³ from 01/01/2021 to 06/29/2021. Similar to the taxi data, the raw data are presented in tabular format. Each data point summarizes the call information, including the longitude and latitude of the location where the call was made.
- **Chicago Taxi Data Data:** Chicago taxi data were collected from Chicago Data portal⁴ from 01/01/2022 to 12/31/2022. Similar to NYC datasets, the raw data are presented in tabular format. Each data point summarizes each taxi trip information, including the longitude and latitude of the location where the passenger was picked up.

¹<https://opendata.cityofnewyork.us/data/>

²<https://citibikenyc.com/system-datafrom>

³<https://data.cityofnewyork.us/Public-Safety/NYPD-Calls-for-Service-Year-to-Date-/n2zq-pubd>

⁴<https://data.cityofchicago.org/Transportation/Taxi-Trips-2022/npd7-ywvj>

The average counts for each geographic level and the corresponding standard deviations are reported in Table 1. We noticed that the standard deviations are rather large. This is because the uneven distribution of data points. Take taxi data for example, upper Manhattan regions (e.g., Inwood) have way fewer taxi rides than central Manhattan.

For NYC, we select four predefined geographic levels, covering lower to finer geospatial resolutions – Public Use Microdata Area (PUMA), Neighborhood Tabulation Areas (NTA), Census Tracts (Tract), and Census Blocks (Block). Their geographic boundaries in 2010 are collected from NYC open data portal. We generated an geographic resolution level – Extreme, which contains areal units that are smaller than Census Block. This geographic resolution is to prepare for the synthesis of individual data records. For Chicago, which has different predefined geographic structures than NYC, we select geographic levels as close as possible to those of NYC – Community Areas (COM), Census Tracts (Tract), and Census Blocks (Block). We also generated an geographic resolution level – Extreme, which contains areal units that are smaller than Census Block. Figure 1 shows the resolutions of five geographic levels in NYC. We construct two types of input data:

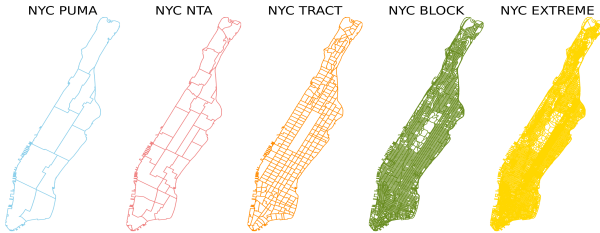


Figure 1: Visualizations of five different geographic levels. PUMA has the most coarse resolution, while EXTREME has the finest resolution.

- **Vector Inputs:** We construct the aggregated hourly count data at the five geographic levels, using the individual records from the datasets. For each hour, we count how many records are located within each areal unit at each geographic level. The vector data is represented as $X_{vec} \in \mathbb{R}^{N \times d}$, where N is the total number of hours, and d is the number of areal units in each geographic level (e.g. $d = 10$ for PUMA; $d=32$ for NTA).
- **Image Inputs:** to disaggregate urban data, we need to model the spatial correlations among the units between coarse and fine geographic level, as well as within each level. Convolutional Neural Networks (CNN) are good at modeling spatial connections. Therefore, we transform each vector input into an image. We plot units at each geographic level. The pixels in each unit takes the value of $\frac{Count\ Value}{\#of\ pixels\ in\ unit}$

For all three NYC datasets, we use the month of June as the test split, the month of May as the validation split, and the rest as training data. For Chicago taxi data, we use the month of December as the test split, November as the validation split, and the rest as training data. The split information is presented in Table 2.

Data	Train	Val	Test
Taxi	2,904	744	720
Bikeshare	2,904	744	720
911 Calls	2,880	744	720
Chicago Taxi	7,296	720	744

Table 2: Count of hourly data records in each split.

4 MODELS

4.1 Baselines Models

As our baseline, we tested several neural models as well as simple, traditional disaggregation methods:

- **Constant Weighting (CW):** a simple method that disaggregates data uniformly over the total number of regions at the finer resolution.
- **Areal Weighting (AW):** a simple method that disaggregates data proportionally to the areas of target regions at the finer resolution. The larger the region, the larger the value it gets.
- **Historical Ratios (HR):** a simple method that disaggregates data based on historical distribution ratios. Unlike AW that disaggregates uniformly, HR calculates the average disaggregation ratios from the source regions to the target regions based on historical data (e.g., training data). The ratios are then applied on unseen data.
- **Feedforward Neural Network (FNN):** a multi-layer feedforward neural network, which models the non-linear spatial connections among the areal units between coarse and fine geographic levels. We name it spatial NN to distinguish it from spatiotemporal NN, which incorporates both spatial and temporal information.
- **Convolutional Neural Network (CNN):** a model with UNet architecture, which takes in image inputs and models the spatial correlations among pixel values.
- **LSTM:** Long Short Term Memory network is a well-known network architecture which is powerful in capturing sequential dependency. We chose $T=5$ as the temporal sequence length based on the study [6].

4.2 Proposed Methods

4.2.1 Chain of Training (COT). Based on preliminary experimental results, we noticed that as we disaggregate into finer geographic regions (e.g., from puma to block compared with fromp puma to nta), the task gets harder thus yielding worse results. We hypothesize that if we can disaggregate in a hierarchical style, the results could be boosted. Therefore, we propose a training approach for disaggregation task, **Chain-of-Training (COT)**, that can be incorporated into any of the training-based models. The idea is simple – when we disaggregate from low to high geographic resolution, we add transitional disaggregation steps by incorporating intermediate geographic dimensions. See Figure 2 for detailed illustration.

The advantage of adding intermediate geographic dimensions is that it makes the model layers interpretable. Additionally, when we have data at the high geographic level, we automatically have data at the intermediate levels, which can be utilized for training purposes. In regular training (e.g., FNN), the objective function is the

Data	PUMA	NTA	TRACT	BLOCK	EXTREME
Taxi	1443.01 (1776.03)	450.94 (689.15)	50.99 (73.26)	3.85 (8.02)	1.27 (3.59)
Bikeshare	189.53 (279.24)	59.23 (97.86)	6.7 (13.06)	0.5 (2.53)	0.17 (1.41)
911 Calls	23.25 (14.22)	7.27 (7.05)	0.82 (1.34)	0.06 (0.32)	0.02 (0.19)
Data	Community	TRACT	BLOCK	EXTREME	-
Chicago Taxi	27.71 (64.61)	2.39 (10.91)	0.06 (1.7)	0.04 (1.35)	-

Table 1: Descriptive statistics of four datasets. The reported numbers are the average counts per geographic region. The standard deviation is in the parenthesis.

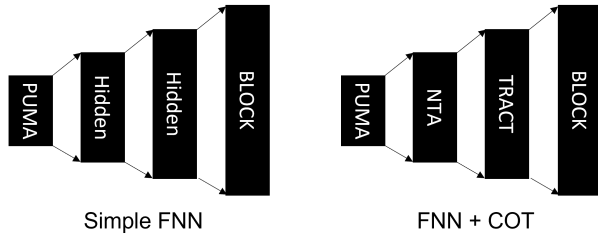


Figure 2: The visualizations show the model architectures to disaggregate from PUMA level to BLOCK level. Left: architecture of a regular feedforward neural network model with two hidden layers. The hidden dimensions could be of any values. Right: The two hidden layers have the dimension sizes that are equal to the count of NTA and TRACT regions.

ℓ_1 loss at the highest geographic level: $\ell_{high} = \frac{1}{N} |\sum X_{high}^{\hat{}} - X_{high}|$. With COT, we also calculate the losses at the intermediate levels and back-propagate them together with the loss at the last layer:

$$\ell_{total} = \ell_{high} + \ell_{intermedite}$$

$$\ell_{intermedite} = \frac{1}{N} |\sum X_{intermedite}^{\hat{}} - X_{intermedite}|$$

We hypothesize that this would be particularly helpful when the disaggregation range is wide (e.g. going from PUMA to BLOCK). Training on those hidden layers could potentially help with the disaggregation results by making improvements step by step.

4.2.2 Reconstruction (REC) Loss. Inspired by [17] in the work of super-resolution, where they generated high-resolution images from low-resolution, and restored the high-resolution images backward to low-resolution. Then the models are jointly trained on the loss calculated from both inputs and outputs. We adapted similar idea in our disaggregation case — together with COT training procedure, we first disaggregate from low to high geographic level, and then re-aggregate back to the low level from our generated high level values. We calculate disaggregation losses at both high and intermediate levels, as well as reconstruction losses. We tested *Full-reconstruction* as shown in Figure 3. For each high geographic level, we reconstruct all possible lower levels beneath it, and take the average at each lower level. The objective function is then:

$$\ell_{total} = \alpha_1 \ell_{PUMA} + \alpha_2 \ell_{NTA} + \alpha_3 \ell_{TRACT} + \alpha_4 \ell_{BLOCK} + \alpha_5 \ell_{EXTREME}$$

For NYC data, the models disaggregate from PUMA level data, into NTA, TRACT, BLOCK, and EXTREME levels. Therefore, we

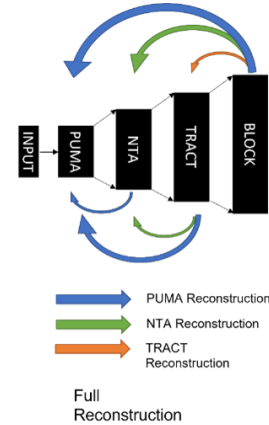


Figure 3: Reconstruction regimes.

have four disaggregation tasks. Likewise, we have three disaggregation tasks for Chicago taxi data, which all start from COM level. We evaluate the results using **Mean Absolute Error (MAE)**. For neural methods, the batch size is 8 and learning rate is $1e-4$. We use early stop setting to prevent over-fitting the training data.

5 EXPERIMENTAL RESULTS

In this section, we present the experimental results of all the models as well as our proposed methods on four datasets.

5.1 Neural Methods Outperform Traditional Methods

For each dataset, the models are trained on the its own training set, and the results are reported on the corresponding test set. The errors are normalized by the area. Consequently, we could compare the results across different disaggregation resolutions. Table 3 presents the quantitative disaggregation results. For the convenience of comparison, we visualize the errors in Figure 4. We have several observations from the visualizations: 1) As the target disaggregation resolution gets finer, the task gets harder, which is supported by the observation that the errors are larger for finer high resolutions. 2) Simple disaggregation methods, such CW and AW, do not perform well across all resolutions in all three datasets. HR, though without any training, improves the performances a lot over the simple methods. 3) Neural methods overall outperform simple methods. However, models that utilize temporal information, in addition

Dataset	Resolutions	CW	AW	HR	FNN	CNN	LSTM
Taxi	PUMA → NTA	1.820705	1.400443	0.463015	0.364603	0.227565	0.209696
	PUMA → TRACT	1.850812	2.055297	0.960405	0.700117	0.592701	0.562141
	PUMA → BLOCK	3.088336	2.963414	1.757388	1.500080	1.509036	1.421459
	PUMA → EXTREME	4.282211	3.907982	2.314584	2.661453	2.242518	-
Bikeshare	PUMA → NTA	0.296892	0.201911	0.107852	0.101145	0.086823	0.089066
	PUMA → TRACT	0.518658	0.490639	0.265565	0.255558	0.241655	0.241166
	PUMA → BLOCK	1.412735	1.354402	0.398009	0.390442	0.386120	0.357188
	PUMA → EXTREME	1.559778	1.523974	0.406618	0.688281	0.445166	-
911 Call	PUMA → NTA	0.030705	0.023857	0.015683	0.016084	0.015639	0.016175
	PUMA → TRACT	0.067976	0.068798	0.054865	0.050578	0.050630	0.050546
	PUMA → BLOCK	0.123104	0.120838	0.101465	0.063181	0.064917	0.062418
	PUMA → EXTREME	0.128736	0.127147	0.105850	0.064858	0.067793	-

Table 3: Disaggregation results traditional and neural-based methods. The unit of the error is count/block/hour.

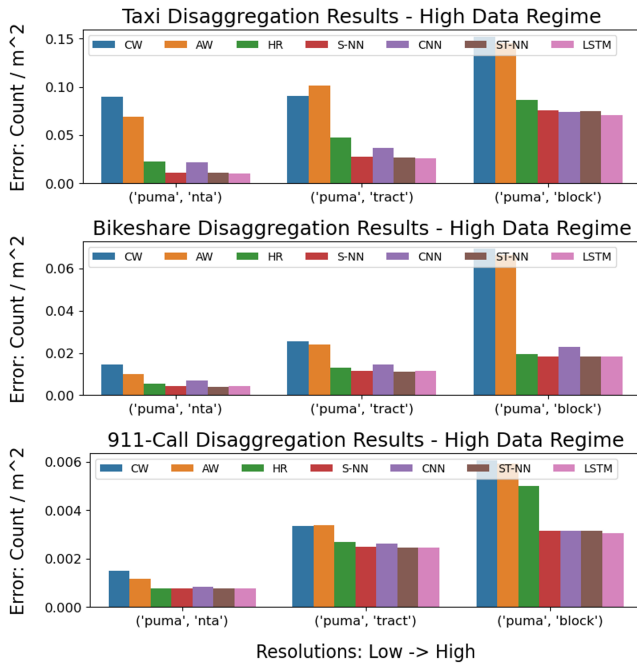


Figure 4: High-regime disaggregation results on three datasets. X-axis shows the disaggregation resolutions. Y-axis shows the error per squared meter. Different colors indicate different models.

to the spatial information, have better performances than those models that only use spatial information. LSTM appears to be the best model out of all.

5.2 COT+Reconstruction Improves Results

We tested the proposed COT-REC method on two models — FNN and LSTM, across all three datasets. The results are presented in Table 4. We noticed that — 1) when the plain models are trained together with COT or both COT and REC, the performances are better than the plain results for most of the disaggregation tasks. With Taxi data, training with both COT and REC improves the

most, while for the rest two datasets, COT alone generates better results. 2) For the cases where the plain models outperform COT and COT-REC, three out of four are disaggregation from PUMA to NTA, which is the easiest task. Additionally, the differences are trivial and statistically insignificant.

6 ABLATION STUDY

In this section, we present two ablation studies about model weighting and different reconstruction schemes.

6.1 Weighted v.s. Unweighted Models

Since we calculate errors at all geographic levels and train the models with all the errors jointly, we need to weight each term in the objective function properly. We observed that the disaggregating from PUMA to EXTREME is a much harder task than from PUMA to NTA. Therefore, the loss term at the EXTREME level would be larger than that at the NTA level. Consequently, the weights for each term in the objective function is determined by the dimension of each geographic level, which up-weights the NTA loss more. To show the effects of proper weighting, we trained models without the weighting and report the results in Table 5. We noticed that when disaggregating from PUMA to NTA, weighting does not provide much benefits, though the differences are still insignificant. For the other two disaggregation tasks, we observed larger improvement with weighted models. The reason is that NTA loss is much smaller than EXTREME loss. Without the weighting, EXTREME loss will dominate the learning process, which counters the idea of enforcing better results at low levels.

6.2 Reconstruction Schemes

In the main text, we reported the results of Full reconstruction. Here we explored two more reconstruction options, namely — *Bridge* reconstruction and *BottomUp* reconstruction. *Bridge* reconstruction only reagggregates lower level values from the adjacent higher level, such as from NTA to PUMA and from BLOCK to TRACT. *BottomUp* reconstruction reagggregates lower level values only from the highest geographic level in the task. We trained the models in the same way as described above. The results are provided in Table 6. *Full* and *BottomUp* reconstruction both provide promising results, though *BottomUp* reconstruction sometimes generates way worse

Dataset	Model	Resolutions	Plain	+COT	+COT, +REC-Full
Taxi	FNN	PUMA → NTA	0.2276	0.2302	0.2328
		PUMA → TRACT	0.5927	0.5752	0.5695
		PUMA → BLOCK	1.5090	1.5023	1.4890
		PUMA → EXTREME	2.2425	2.2328	2.2025
	LSTM	PUMA → NTA	0.2097	0.2101	0.2149
		PUMA → TRACT	0.5621	0.5448	0.5429
Bike	FNN	PUMA → NTA	0.0868	0.0806	0.0815
		PUMA → TRACT	0.2417	0.2314	0.2321
		PUMA → BLOCK	0.3861	0.3675	0.3913
		PUMA → EXTREME	0.4452	0.4224	0.4456
	LSTM	PUMA → NTA	0.0891	0.0830	0.0829
		PUMA → TRACT	0.2412	0.2335	0.2316
911-Call	FNN	PUMA → NTA	0.0156	0.0156	0.0157
		PUMA → TRACT	0.0506	0.0502	0.0531
		PUMA → BLOCK	0.0649	0.0638	0.0884
		PUMA → EXTREME	0.0678	0.0667	0.0952
	LSTM	PUMA → NTA	0.0162	0.0156	0.0156
		PUMA → TRACT	0.0505	0.0502	0.0527
		PUMA → BLOCK	0.0624	0.0625	0.0946

Table 4: Disaggregation results of neural-based methods and our proposed COT-REC method. The unit of the error is count/block/hour.

Dataset	Model	Resolutions	Plain	+COT	+COT, +REC-Full
Taxi	Unweighted FNN	PUMA → NTA	0.2276	0.2313	0.2308
		PUMA → TRACT	0.5927	0.5773	0.5715
		PUMA → BLOCK	1.5090	1.5157	1.5884
		PUMA → EXTREME	2.2045	2.2328	2.3131
	Weighted FNN	PUMA → NTA	0.2276	0.2302	0.2328
		PUMA → TRACT	0.5927	0.5752	0.5695
		PUMA → BLOCK	1.5090	1.5023	1.4890
		PUMA → EXTREME	2.2425	2.2328	2.2025

Table 5: Disaggregation results of weighted and unweighted models. The unit of the error is count/block/hour.

results than the plain model (e.g. PUMA to TRACT). Therefore, *Full* reconstruction is relatively more stable. *Bridge* reconstruction improves over the plain model results, but not as good as the other two methods.

7 DISCUSSION

In this work, we aim to synthesize fine-grained, high resolution urban data, by breaking down aggregated urban data at coarse, low resolution geographic units. The goal is to increase the usability and realize the values as much as possible of highly aggregated urban data. To address the issue of simplicity of some traditional disaggregation methods – 1) we experimented with numerous neural-based models that are capable of modeling intricate non-linear relationships among features. Neural methods can also leverage both spatial and temporal information concurrently. We showed that all neural methods perform better than traditional disaggregation methods. Incorporating the temporal information further enhances the results. 2) We proposed a training approach for disaggregation task, Chain-of-Training (COT), that can be incorporated into any of the training-based models. COT adds transitional disaggregation

steps by incorporating intermediate geographic dimensions, which enhances the predictions at low geographic level and boosts the results at higher levels. 3) We adapted the idea of reconstruction (REC) from super-resolution domain in our disaggregation case – after disaggregating from low to high geographic level, we then re-aggregate back to the low level from our generated high level values. Both strategies improved disaggregation results on three datasets and two cities we tested on.

REFERENCES

- [1] Rohan Arambepola, Tim C. D. Lucas, Anita K. Nandi, Peter W. Gething, and Ewan Cameron. 2020. A simulation study of disaggregation regression for spatial disease mapping. *Statistics in Medicine* 41 (2020), 1 – 16.
- [2] Alexis J. Comber and Wen Zeng. 2019. Spatial interpolation using areal features: A review of methods and opportunities using new forms of data with coded illustrations. *Geography Compass* (2019).
- [3] Pierre Deville, Catherine Linard, Samuel Martin, Marius Gilbert, Forrest R. Stevens, Andrea E. Gaughan, Vincent D. Blondel, and Andrew J. Tatem. 2014. Dynamic population mapping using mobile phone data. *Proceedings of the National Academy of Sciences of the United States of America* 111, 45 (Sept. 2014), 15888–15893. <https://doi.org/10.1073/pnas.1408439111>
- [4] M F Goodchild, Luc Anselin, and Uwe Deichmann. 1993. A Framework for the Areal Interpolation of Socioeconomic Data. *Environment and Planning A* 25 (1993), 383 – 397.

Dataset	Model	Resolutions	Plain	+COT	+COT, +REC- BottomUp	+COT, +REC- Bridge	+COT, +REC- Full
Taxi	FNN	PUMA → NTA	0.2276	0.2302	0.2328	0.2328	0.2328
		PUMA → TRACT	0.5927	0.5752	0.6197	0.5780	0.5695
		PUMA → BLOCK	1.5090	1.5023	1.4908	1.5203	1.4890
		PUMA → EXTREME	2.2425	2.2328	2.1683	2.2911	2.2025
	LSTM	PUMA → NTA	0.2097	0.2101	0.2149	0.2149	0.2149
		PUMA → TRACT	0.5621	0.5448	0.5405	0.5412	0.5429
		PUMA → BLOCK	1.4215	1.4136	1.3926	1.4033	1.3926

Table 6: Disaggregation results of different reconstruction schemes. The unit of the error is count/block/hour.

- [5] Ben Green, Gabe Cunningham, Ariel Ekblaw, Paul M. Kominers, Andrew Linzer, and Susan P. Crawford. 2017. Open Data Privacy: A risk-benefit, process-oriented approach to sharing and protecting municipal data.
- [6] Bin Han and Bill Howe. 2023. Adapting to Skew: Imputing Spatiotemporal Urban Data with 3D Partial Convolutions and Biased Masking. arXiv:2301.04233 [cs.CV]
- [7] João Monteiro, Bruno Martins, Patricia Murrieta-Flores, and João M. Pires. 2019. Spatial Disaggregation of Historical Census Data Leveraging Multiple Sources of Ancillary Information. *ISPRS International Journal of Geo-Information* 8, 8 (2019). <https://doi.org/10.3390/ijgi8080327>
- [8] João Monteiro, Bruno Martins, Patricia Murrieta-Flores, and João M. Pires. 2019. Spatial Disaggregation of Historical Census Data Leveraging Multiple Sources of Ancillary Information. *ISPRS International Journal of Geo-Information* 8, 8 (2019). <https://doi.org/10.3390/ijgi8080327>
- [9] João Monteiro, Bruno Martins, and João Pires. 2018. A hybrid approach for the spatial disaggregation of socio-economic indicators. *International Journal of Data Science and Analytics* 5 (03 2018). <https://doi.org/10.1007/s41060-017-0080-z>
- [10] Yue Qiu, Xuesheng Zhao, Deqin Fan, and Songnian Li. 2019. Geospatial Disaggregation of Population Data in Supporting SDG Assessments: A Case Study from Deqing County, China. *ISPRS Int. J. Geo Inf.* 8 (2019), 356.
- [11] Forrest R. Stevens, Andrea E. Gaughan, Catherine Linard, and Andrew J. Tatem. 2015. Disaggregating Census Data for Population Mapping Using Random Forests with Remotely-Sensed and Ancillary Data. *PLOS ONE* 10, 2 (02 2015), 1–22. <https://doi.org/10.1371/journal.pone.0107042>
- [12] CE Utazi, Julia Thorley, V. Alegana, Mjgs Ferrari, Kristine Nilsen, Saki Takahashi, C. Jessica E. Metcalf, Justin Lessler, and AJ Tatem. 2018. A spatial regression model for the disaggregation of areal unit based data to high-resolution grids with application to vaccination coverage mapping. *Statistical Methods in Medical Research* 28 (2018), 3226 – 3241.
- [13] Stefaan Verhulst, Andrew Young, Andrew Zahuranec, Susan Ariel Aaronson, Ania Calderon, and Matt Gee. 2020. The emergence of a third wave of open data. (2020).
- [14] Patrick Vogel, Torsten Greiser, and Dirk Christian Mattfeld. 2011. Understanding bike-sharing systems using data mining: Exploring activity patterns. *Procedia-Social and Behavioral Sciences* 20 (2011), 514–523.
- [15] N. A. Wardropa, W. C. Jochem, T. J. Birda, H. R. Chamberlaina, David J. Clarkea, D. Kerra, Lars Bengtssona, S. Juranc, V. Seamand, and A. J. Tatem. 2018. Spatially disaggregated population estimates in the absence of national population and housing census data.
- [16] Haiyang Yu, Zhihai Wu, Shuqin Wang, Yunpeng Wang, and Xiaolei Ma. 2017. Spatiotemporal recurrent convolutional networks for traffic prediction in transportation networks. *Sensors* 17, 7 (2017), 1501.
- [17] Yuan Yuan, Siyuan Liu, Jiawei Zhang, Yongbing Zhang, Chao Dong, and Liang Lin. 2018. Unsupervised Image Super-Resolution Using Cycle-in-Cycle Generative Adversarial Networks. In *2018 IEEE/CVF Conference on Computer Vision and Pattern Recognition Workshops (CVPRW)*. 814–81409. <https://doi.org/10.1109/CVPRW.2018.00113>